# RESULTS ON HADRONIC DECAYS OF THE $Z$ BOSON AT THE SLC

**Paul Dauncey** *
Department of Physics and Astronomy
The Johns Hopkins University
Baltimore, Maryland, 21218, USA

ABSTRACT

Results on properties of the hadronic decays of the $Z$ boson observed with the Mark II detector at the SLC are presented. Event shape variables and inclusive charged particle distributions have been corrected for detector effects and are compared with lower energy $e^+e^-$ experiments and hadron production models. The $Z$ boson data are consistent with expectations. A measurement of the strong coupling constant, $\alpha_s$, has been made from the differential jet multiplicities using both the $Z$ data and Mark II data at 29 GeV centre-of-mass. The results are consistent with the running of the coupling constant with centre-of-mass energy, as expected by QCD.

* Representing the Mark II Collaboration

## INTRODUCTION

In this paper, we present data from hadronic decays of the $Z$ boson. The data were taken with the Mark II detector at the SLAC $e^+e^-$ Linear Collider (SLC) running at several centre-of-mass energies ($E_{cm}$) near the $Z$ boson resonance peak at 91.1 GeV[1]. The data correspond to a total integrated luminosity of 19.7 $nb^{-1}$. Comparisons with lower energy data[2),3),4)] are presented, particularly with measurements at 29 GeV $E_{cm}$ taken with essentially the same detector. This allows us to compare the data at 29 GeV and 91 Gev without potentially large systematic differences.

## DETECTOR, TRIGGERS AND EVENT SELECTION

The Mark II detector has been described elsewhere[5]. The triggering was performed with both charged and neutral energy triggers which had considerable redundency. The combined overall efficiency for hadronic events was 99.8 % and hence gave an unbiased sample of events.

The events were selected on the basis of charged tracks reconstructed in the tracking chambers and neutral energy showers in the calorimeters. Hadronic events used in this analysis were required to have at least 7 well-constructed charged tracks and a total visible energy from charged tracks and neutral energy of at least 0.5 $E_{cm}$. The total number of events passing these cuts was 381. The selection efficiency for these cuts was estimated from Monte Carlo simulations to be $0.77 \pm 0.01$.

The background contributions from beam-gas scattering, lepton pairs and two-photon production were estimated to be small ($< 0.5$ events) and are neglected. The distributions presented here were all corrected using bin-by-bin multiplicative correction factors calculated from Monte Carlo simulations. Corrections were made for detector effects, machine-induced backgrounds, initial state radiation and $K^0_S$ and $\Lambda$ decays. The correction factors were typically $\sim 1.2$.

Comparisons of the $Z$ boson data with several QCD-based models[2] are presented here. The models used were the Lund parton shower model with string fragmentation (Lund 6.3 Shower), the Webber-Marchesini parton shower model with cluster fragmentation (Webber 4.1) and the parton shower model of Gottschalk and Morris (Caltech-II 86). The Lund matrix element model is not shown as it cannot be correctly extrapolated from 29 GeV to 91 GeV without retuning[6]. These models were tuned to the 29 GeV data[2] and have not been refitted to the $Z$ data. Hence, all the results from models presented here are predictions extrapolated from 29 GeV.

## GLOBAL EVENT SHAPE DISTRIBUTIONS

The event shape variables[2] sphericity (S) and aplanarity (A) are commonly used to represent event shapes. The corrected distributions of these quantities are shown in figures 1 and 2 respectively. Also shown are the predictions of the three QCD-based models. It is seen that the models represent the data well, at the level of the available statistics.

The mean sphericity was determined to be $\langle S \rangle = 0.078 \pm 0.005$ and the mean aplanarity to be $\langle A \rangle = 0.0117 \pm 0.0007$. These values are shown in figure 3 as a function of $E_{cm}$, together with the means from lower energy $e^+e^-$ experiments and the predictions of the Lund 6.3 Shower model. The other two models have a very similar energy dependence. The 91 GeV data are seen to agree well with expectations from both the lower energy data and the model.

## INCLUSIVE CHARGED PARTICLE DISTRIBUTIONS

The mean charged multiplicity was determined by a matrix unfold technique to be 20.1 ± 1.0 ± 1.0. This value is shown in figure 4 together with values from lower energy $e^+e^-$ experiments and the Lund 6.3 Shower model predictions. The data are consistent with expectations.

The momentum distribution of the charged particles is shown in figure 5 in terms of the scaled variable $x$, where $x = 2p/E_{cm}$. Also shown are the three model predictions. Again, the models agree with the data. The dependence of the different $x$ bins on $E_{cm}$ is shown in figure 6 along with lower energy data and the Lund 6.3 Shower model predictions. The scaling violations observable for low $x$ ($x < 0.1$) are a result of mass and phase space effects. The high $x$ scaling violations are thought to arise from QCD radiation and the fact that the data are consistent with the QCD-based model expectations supports this view.

The distributions for the momentum transverse to the axes of the sphericity tensor, both in ($p_{\perp in}$) and out ($p_{\perp out}$) of the event plane, are shown in figures 7. Also shown are the Mark II data from 29 GeV and the predictions of the models. A clear increase in transverse momentum at 91 GeV compared with 29 GeV is seen for both $p_{\perp in}$ and $p_{\perp out}$ in the perturbative region ($p_\perp \geq 1$ GeV/c). In contrast, the distributions show little difference in the low $p_\perp$ region, where $E_{cm}$-independent fragmentation effects are expected to dominate.

The corrected mean square values were measured to be $< p_{\perp in} >= 0.70 \pm 0.05$ (GeV/c)$^2$ and $< p_{\perp out} >= 0.121 \pm 0.005$ (GeV/c)$^2$. These are shown in figure 8 together with the lower energy data and the Lund 6.3 Shower model. The high energy data agree well with expectations from the lower energy data, but is slightly above the Lund prediction. However, this is not a significant difference with the present level of statistics.

## JET MULTIPLICITY AND THE RUNNING STRONG COUPLING CONSTANT

The JADE jet algorithm[3] was used to find the number of jets in each event as a function of the invariant mass required to define the jets as resolved. For each invariant mass cut, the fractions of events which had $n$ resolvable jets, ($f_n$), were found, where $n$ was 2, 3, 4 or 5. These are shown in figure 9 in terms of the variable $y_{cut}$, where $y_{cut} = m^2_{cut}/E^2_{cm}$ and $m_{cut}$ is the minimum allowed invariant mass of any two jets. Also shown are the Lund 6.3 Shower model predictions, which agree very well with the measured jet fractions.

These fractions, $f_n$, could, in principle, be fitted to a QCD calculation to determine a value of $\alpha_s$. However, the definition of the fractions means that all the data points in figure 9 are highly correlated, as each contains all the events of the points at higher values of $y_{cut}$. To overcome this problem, the variable $y_3$ was defined as the value of $y_{cut}$ which caused an event to change from being resolvable into 3 jets to being resolvable into only 2. The distribution of the $y_3$ values, $g(y_3)$, contains only one contribution per event and so is easier to handle statistically. This distribution of $y_3$ is shown in figure 10a, along with analytic curves from a second order matrix element calculation[7]. A similar analysis of the Mark II data at 29 GeV is shown in figure 10b. Note that these curves are parton level calculations while the data values have obviously been determined using the observed hadrons. No explicit correction has been made, but the effects of hadronisation have been included in the systematic errors and are ±5% at 91 GeV and ±10% at 29 GeV. The data were fitted to the

analytic QCD calculation for $y_3$ values between 0.04 and 0.14 at both energies separately. The lower end of this $y_3$ range was chosen as hadronisation effects become large for smaller values. The upper end was chosen as the analytic calculation does not extend to higher values of $y_3$. The fitted values of $\alpha_s$, choosing the renormalisation point to be $Q^2 = E_{cm}^2$, were

$$\alpha_s = 0.123 \pm 0.009 \pm 0.005 \quad (91 \text{ GeV})$$

$$\alpha_s = 0.149 \pm 0.002 \pm 0.007 \quad (29 \text{ GeV})$$

The values of $\Lambda_{\overline{MS}}$ calculated from the above, using the usual approximate solution of the Renormalisation Group Equation[8], were

$$\Lambda_{\overline{MS}} = 0.29 \, ^{+0.17}_{-0.12} \, ^{+0.11}_{-0.06} \text{ GeV} \quad (91 \text{ GeV})$$

$$\Lambda_{\overline{MS}} = 0.28 \, ^{+0.02}_{-0.02} \, ^{+0.08}_{-0.07} \text{ GeV} \quad (29 \text{ GeV})$$

These systematic errors do not include a contribution arising from the renormalisation point ambiguity. The values of $\Lambda_{\overline{MS}}$ are in very good agreement and so demonstate that the change in $\alpha_s$ observed between 29 and 91 GeV is consistent with expectations from QCD.

## SUMMARY

We have measured properties of hadronic events from $Z$ boson decays. The properties of the events agree with expecations from both the lower energy data and the predictions of the QCD-based models. The values of $\alpha_s$ determined from the jet multiplicities at 29 and 91 GeV show $\alpha_s$ is running, consistent with QCD predicitions.

## REFERENCES

1) G. S. Abrams *et al.*, Phys. Rev. Lett. **63** (1989) 724; B. Adeva *et al.*, Phys. Lett. **B231** (1989) 509; D. Decamp *et al.*, Phys. Lett. **B231** (1989) 519; M. Z. Akrawy *et al.*, Phys. Lett. **B231** (1989) 530; P. Aarnio *et al.*, Phys. Lett. **B231** (1989) 539
2) A. Peterson *et al.*, Phys. Rev. **D37** (1988) 1
3) W. Bartel *et al.*, Z. Phys. **C33** (1986) 23; S. Bethke *et al.*, Z. Phys. **C43** (1989) 325
4) All other lower energy data shown here are to be found in; C. Bacci *et al.*, Phys. Lett. **B86** (1979) 234; Ch. Berger *et al.*, Phys. Lett. **B95** (1980) 313; B. Niczyporuk *et al.*, Z. Phys. **C9** (1981) 1; J. L. Siegrist *et al.*, Phys. Rev. **D26** (1982) 969; M. S. Alam *et al.*, Phys. Rev. Lett. **49** (1982) 357; Ch. Berger *et al.*, Z. Phys. **C12** (1982) 297; W. Bartel *et al.*, Z. Phys. **C20** (1983) 187; M. Althoff *et al.*, Z. Phys. **C22** (1984) 307; D. Bender *et al.*, Phys. Rev. **D31** (1985) 1; S. Bethke *et al.*, Phys. Lett. **B213** (1988) 235; W. Braunschweig *et al.*, Z. Phys. **C41** (1988) 359; W. Braunschweig *et al.*, Phys. Lett. **B214** (1988) 286; I. H. Park *et al.*, Phys. Rev. Lett. **62** (1989) 1713; H. J. Behrend *et al.*, DESY preprint 89-019; Y. Li, private communication, KEK preprints 89-34, 89-149
5) G. Abrams *et al.*, Nucl. Inst. Meth. **A281** (1989) 55
6) G. S. Abrams *et al.*, Phys. Rev. Lett. **64** (1990) 1334
7) G. Kramer and B. Lampe, Fortschr. Phys. **37** (1989) 161
8) M. Aguilar-Benitez *et al.*, Phys. Lett. **B170** (1986) 78

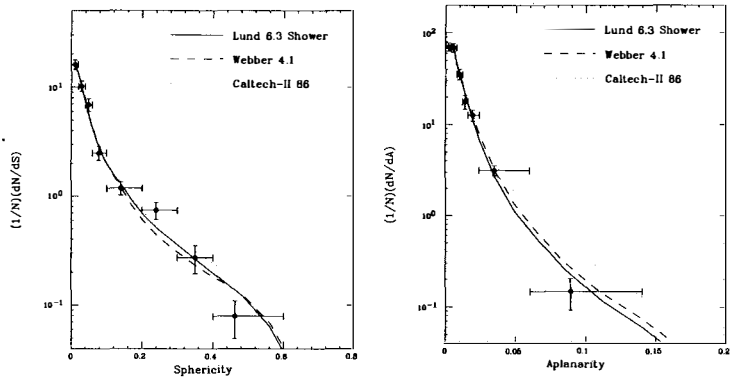


Figure 1) Distribution of sphericity at 91 GeV. The data points are shown with errors, the lines are the predictions of QCD-based models.

Figure 2) Distribution of aplanarity at 91 GeV. The data points are shown with errors, the lines are the predictions of QCD-based models.

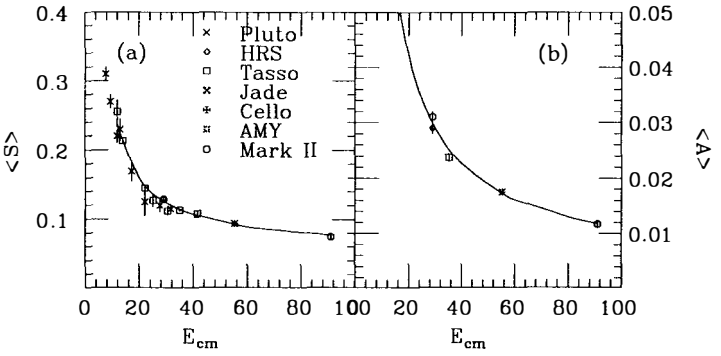


Figure 3) Means of a) sphericity and b) aplanarity as a function of $E_{cm}$. The line is the prediction of the Lund 6.3 Shower model.

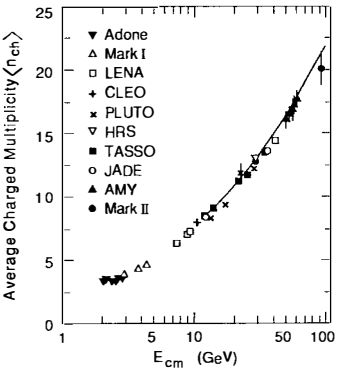


Figure 4) Mean charged multiplicity as a function of $E_{cm}$. The line is the prediction of the Lund 6.3 Shower model.

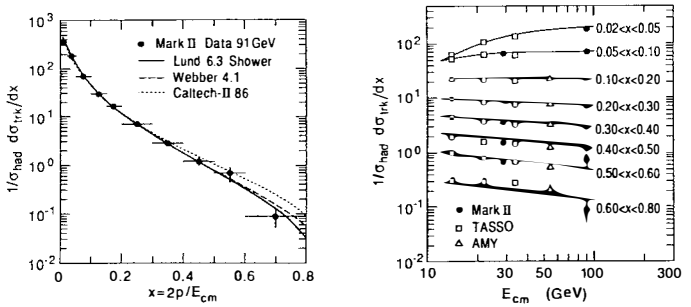


Figure 5) Distribution of $x = 2p/E_{cm}$ at 91 GeV. The data points are shown with errors, the lines are the predictions of QCD-based models.

Figure 6) Values of inclusive $x$ distribution for several bins of $x$ as a function of $E_{cm}$. The line is the prediction of the Lund 6.3 Shower model.

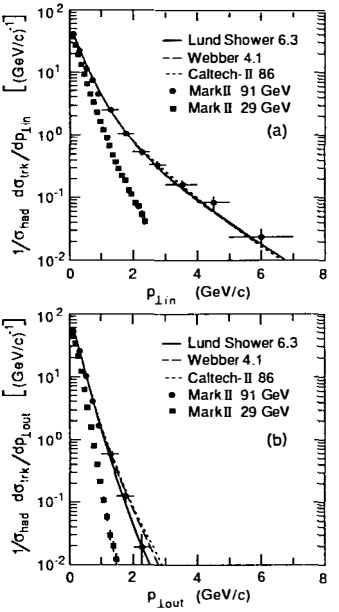


Figure 7) Distribution of a) $p_{\perp in}$ and b) $p_{\perp out}$ at 91 GeV. The data points are shown with errors, the lines are the predictions of QCD-based models. Also shown are the Mark II data points at 29 GeV.

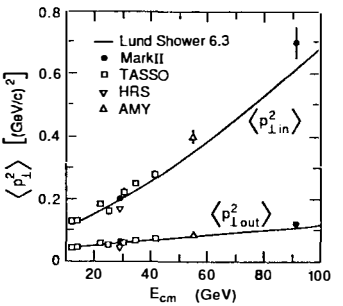


Figure 8) Mean of $p_{\perp in}^2$ and $p_{\perp out}^2$ as a function of $E_{cm}$. The lines are the predictions of the Lund 6.3 Shower model.

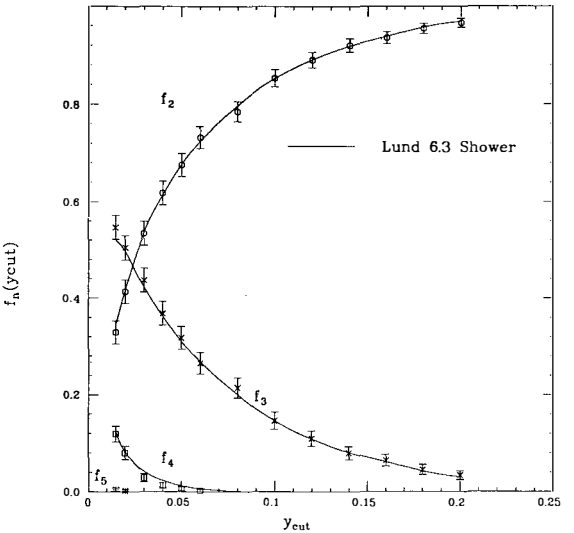


Figure 9) Fractions of multi-jet events, $f_n$, as a function of the invariant mass cutoff parameter, $y_{cut}$. The lines are the predictions of the Lund 6.3 Shower model.

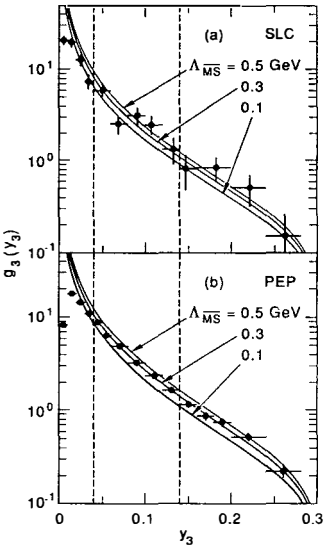


Figure 10) Distribution of the variable $y_3$ (see text) for a) 91 GeV and b) 29 GeV. The lines are analytic calculations from reference 7).